Bioorganic Chemistry 92 (2019) 103295

Contents lists available at ScienceDirect

Bioorganic Chemistry

journal homepage: www.elsevier.com/locate/bioorg

A novel adaptive fluorescent probe for cell labelling

Anca G. Coman[a], Anca Paun[a], Codruta C. Popescu[a], Niculina D. Hădade[b], Anamaria Hanganu[c], Gabriela Chiritoiu[d], Ileana C. Farcasanu[a,*], Mihaela Matache[a,*]

[a] University of Bucharest, Faculty of Chemistry, Department of Organic Chemistry, Biochemistry and Catalysis, Research Centre of Applied Organic Chemistry, 90-92 Panduri Street, RO-050663 Bucharest, Romania
[b] Faculty of Chemistry and Chemical Engineering, Supramolecular Organic and Organometallic Chemistry Centre, "Babes–Bolyai" University, 11 Arany Janos Str., RO-400028 Cluj-Napoca, Romania
[c] Institute of Organic Chemistry "C.D. Nenitescu" of the Romanian Academy, 202B Spl. Independentei, 060023 Bucharest, Romania
[d] Institute of Biochemistry of the Romanian Academy, 296 Spl. Independentei, 060031 Bucharest, Romania

ARTICLE INFO

Keywords:
N-acylhydrazone
Synthesis
Fluorescence
Endoplasmic reticulum
Cell labelling

ABSTRACT

In this study we describe the synthesis and characterisation of a new hydrazone-based fluorescent compound that is able to selectively label the endoplasmic reticulum (ER) in yeast and mammalian living cells. The fluorescence properties of the compound depended on the DMSO/water ratio and on the pH. NMR experiments allowed determination of the conformation adopted in various environments. Apart from the convenient synthetic procedure, our compound displays low cell toxicity and blue emission compatible with filters routinely used in fluorescence microscopy.

1. Introduction

N-acylhydrazones have drawn attention as model compounds suitable to study adaptive systems [1] and molecular switches [2] as result of the controlled dynamic, but fairly stable character of the hydrazone bond, which can be easily prepared by condensation between carbonyls and *N*-acylhydrazines. Additionally, *N*-acylhydrazones are important players in coordination and supramolecular chemistry, in the synthesis of metal-ion complexes and coordination polymers [3] or in synthetic organic chemistry as precursors for oxadiazoles [4]. Hydroxy-bis-*N*-acylhydrazones, bearing numerous coordinating sites, were reported to act as good ligands for copper, zinc, molybdenum or lanthanides [5] yielding complexes that can be further used as catalysts for alcohol oxidations [6] or as fluorescent sensors for zinc(II) (in living cells) or pyrophosphate ions [7] Similar compounds were also found to form luminescent gels [8] with multiple colour emissions, as result of the aggregation occurring in aqueous dilutions of organic solvents. We have previously shown [8a] that molecules of type **I** (Fig. 1) behave as switchable-light emissive molecules triggered by light and/or solvent, through Excited State Intramolecular Proton Transfer (ESIPT) [9] and/or Aggregation Induced Emission (AIE) [10], by changes in conformation.

In light of our findings, corroborated with the structural simplicity, but also with the versatility of these compounds we continued to scan the behaviour of such molecules, in an attempt to find other useful applications. Numerous synthetic fluorescent small molecules can be used for selective visualization of the individual cell organelles [11]. Thus, xanthenes, dipyrolomethanes, cyanines [12], various substituted olefins and pyran derivatives or C=N bond containing molecules (i.e. imines, hydrazones) [13] were reported as good cell labelling markers. Whereas mitochondria or lysosome-targeting fluorescent probes are frequently encountered [11f], reports concerning selective endoplasmic reticulum (ER)-labelling are less numerous [11e]. The most common selective ER-targeting dyes include positively charged cyanines or xanthene derivatives [11e] as well as some recently reported rhodols, metal-ion complexes or imine-based analogues [14].

In this context, we present here synthesis of compound **1**, investigation of the physical and chemical properties (the responses to various physical and chemical stimuli) as well as its particular ability to selectively label the endoplasmic reticulum (ER) in yeast and mammalian cells.

2. Materials and methods

2.1. Organic synthesis

General experimental information. All commercial reactive and reagents were used without further purification. Thin layer

* Corresponding authors.
E-mail addresses: ileana.farcasanu@chimie.unibuc.ro (I.C. Farcasanu), mihaela.matache@g.unibuc.ro (M. Matache).

https://doi.org/10.1016/j.bioorg.2019.103295
Received 20 May 2019; Received in revised form 11 September 2019; Accepted 16 September 2019
Available online 17 September 2019
0045-2068/

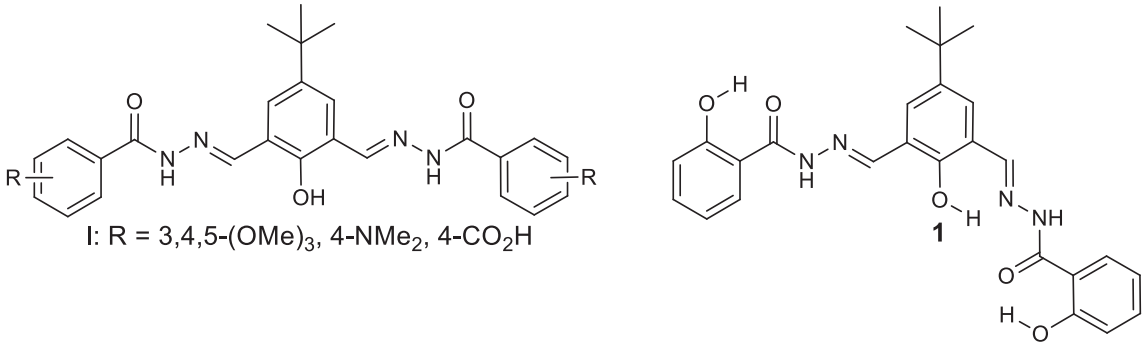

Fig. 1. Structure of previously described *N*-acylhydrazones I behaving as switchable-light emissive molecules and structure of compound 1 used in this study.

chromatography (TLC) was performed on silica gel 60 coated aluminium F254 plates with visualization by UV irradiation at 254 and 365 nm. The NMR spectra were recorded on Bruker Advance Ultrashield Plus spectrometer operating at 500 MHz for ^{1}H and 125 MHz for ^{13}C. High resolution mass spectrum was recorded on Thermo Scientific (LTQ XL Orbitrap) spectrometer, in positive ion mode, using APCI technique. Melting points were determined in open capillary tubes using a STUART SMP3 electric melting point apparatus and are uncorrected.

(*N′,N″E,N′,N″E*)-*N′,N″*-(5-*tert*-butyl-2-hydroxy-1,3-phenylene)bis(methan-1-yl-1-ylidene)bis(2-hydroxybenzohydrazide) 1. A mixture of 5-*tert*-butyl-2-hydroxyisophthalaldehyde (1 eq., 0.365 mmol, 75 mg) and 2-hydroxybenzohydrazide (2 eq., 0.73 mmol, 111 mg) were dissolved in DMSO (up to approx. 0.1 M concentration, 3.5 mL) and a few drops of trifluoroacetic acid were added. The reaction mixture was heated at 100 °C for 4 h and left at room temperature overnight (12 h). Water was added to the reaction mixture (90% v/v, 31.5 mL) and the resulting precipitate was filtered, washed with water and dried. Light-yellow solid. Yield 80% (131 mg). *m.p.* 150–153 °C. R_f = 0.26 (silica, EtOAc). ^{1}H RMN (500.13 MHz, DMSO-d_6): δ = 12.34 (s, 1H, O*H*), 12.80 (s, 2H, N*H*), 11.76 (s, 2H, O*H*), 8.79 (s, 2H, C*H*N), 7.90 (d, 2H, ^{3}J = 7.7 Hz H_7), 7.78 (s, 2H, H_3), 7.46 (t, 2H, ^{3}J = 7.5 Hz, H_9), 7.00–6.96 (overlapped peaks, 4H, H_8/H_{10}), 1.34 (s, 9H, *t*Bu) ppm. ^{13}C NMR (125.77 MHz, DMSO-d_6): δ = 165.0 (C═O), 159.4 (C-6), 155.3 (C-2), 147.7 (C-5), 142.2 (C-4), 134.4 (C-9), 129.1 (C-7), 127.6 (C-3), 119.9 (C-1), 119.5 (C-8/C-10), 117.7 (C-8/C-10), 116.3 (C-11), 34.4 (*C*-*t*Bu), 31.6 (*t*Bu). HRMS (APCI, +) (*m/z*): calcd. for $C_{26}H_{27}N_4O_5$ [M + H]$^{+}$: 475.1976, found: 475.1969.

2.2. Absorption and emission spectroscopy

2.2.1. UV–VIS spectroscopy

Absorption spectra were recorded with a Jasco V-630 spectrophotometer, using 10 mm quartz cell. Stock solutions of compound were prepared in DMSO (10^{-2} mol L^{-1}), diluted to 2×10^{-5} mol L^{-1} using DMSO and water (10%, 25%, 50%, 75%, 90% v/v).

2.2.2. Fluorescence spectroscopy

Fluorescence spectra in solution were recorded with a Thermo Scientific Varioskan Flash spectral scanning multimode reader. The spectra were recorded in suitable plates using 5 nm excitation and emission slits for all measurements. Stock solutions of compound were prepared in DMSO (10^{-2} mol L^{-1}), diluted to 10^{-4} mol L^{-1} using DMSO and water (10%, 25%, 50%, 75%, 90% v/v). The solid state fluorescence spectra were recorded using a JASCO FP 8300 spectrofluorometer.

2.3. Cell staining

2.3.1. Yeast strain and growth

The *S. cerevisiae* strains used in this study was BY4741 (*MATa; his3Δ1; leu2Δ0; met15Δ0; ura3Δ0*) obtained from EUROSCARF (European *S. cerevisiae* Archive for Functional Analysis, www.euroscarf.de). Yeast cells were propagated, grown and maintained in YPD medium (1% yeast extract, 2% polypeptone, 2% glucose) or synthetic complete medium SD (synthetic complete, 0.17% yeast nitrogen base without amino acids, 0.5% $(NH_4)_2SO_4$, 2% glucose, supplemented with the essential amino acids). For growth assay, cells from an overnight pre-culture were inoculated in fresh medium at density of 10^5 cells/mL (OD_{600} = 0.01). Cells were grown with agitation (30 °C, 200 rpm) to OD_{600} = 0.1, which corresponded to approximately 10^6 cells/mL. The cell viability was checked by staining with methylene blue (Roth, Germany) and only populations with viability > 99% were used further. At this point (considered time 0) compound **1** was added to the desired concentration from a 10^{-2} M sterile stock DMSO solution. Cell growth in liquid media was monitored by measuring OD_{600} as a function of time, recorded in a plate reader equipped with thermostat and shaker (Varioskan, Thermo Fisher Scientific, Vantaa, Finland).

2.3.2. CCD fibroblasts and HeLa cells cultivation

CCD fibroblasts and HeLa cells were cultivated in DMEM supplemented with 10% FBS (fetal bovine serum). The cells were grown on cover glass at 60–70% confluency and transfected or not with *EDEM1::YFP*. Shortly, the cells were incubated 24–48 h with a mix of Lipofectamine 2000:DNA (2.5:1 ratio) following the manufacturer's protocol. Post transfection the cells were incubated with 10^{-4} M compound **1** in DMSO for 2 h and immediately visualized by microscopy.

2.3.3. MTS assay

The cytotoxicity of **1** was evaluated by MTS assay for which CCD fibroblasts and HeLa cells were plated in 96 well plates as 4 technical replicates. Adhered cells were incubated with **1** for various time periods (0 h, 1 h, 2 h, 4 h and 6 h), washed 2 times with PBS (Phosphate buffered saline) and incubated with a mix of media: MTS reagent (5:1 ratio), for 2 h. Absorbance of soluble brown formazan, product of MTS bioreduction, was measured at 490 nm. Percentage of cellular viability, determined as ratio of non-treated cells absorbance to **1** treated cells absorbance, was represented as a line chart.

2.3.4. Staining protocol and fluorescence microscopy of yeast cells

Exponentially growing yeast cells (10^6 cells/mL) were treated with 10^{-2} M **1** in DMSO (100 v/1 v), 1 mg mL^{-1} in ethanol $DiOC_6$ (100 v/1 v) or both, for cross-staining. Cells were incubated for at least 30 min (30 °C, 200 rpm) before being harvested and washed in MES/Tris (pH 6.8) to be visualized by fluorescence microscopy. Live yeast cells were examined with an Olympus fluorescent microscope system (Olympus BX53, Japan) equipped with a HBO-100 mercury lamp and an Olympus DP73 camera. To detect the signals of **1**, a DAPI filter set (excitation filter 340–390, dichromatic mirror 410, emission filter 420) was used. To detect the $DiOC_6$ signals, a FITC filter set (excitation filter 460–480, dichromatic mirror 585, emission filter 510–550) was used.

2.3.5. Confocal microscopy

Confocal images were acquired with Zeiss LSM 710 laser scanning confocal microscope (Carl Zeiss, Oberkochen, Germany), in a multitrack mode using a single or dual excitation (Diode 405 excitation for the blue dye and Argon 488 for the YFP), with a pinhole of 1.0 Airy Units. Images were processed with Adobe Photoshop CS. The colocalization analyses were done on raw images using Colocalization measurement feature of Zen 2010 software. The reported values are representative and reflect the average colocalization coefficients.

3. Results

3.1. Synthesis and photophysical properties of compound 1

Synthesis of **1** was achieved through a condensation reaction between the corresponding aldehyde and hydrazide, under acid catalysis (see SI). Preliminary assays indicated good solubility in polar solvents such as DMSO, DMF or THF, unlike most hydrazone-based compounds, which have a well-known poor solubility. Absorption spectroscopy in DMSO indicated maxima at λ_{max} = 325 nm and λ_{max} = 370 nm, which could be assigned to π-π* transitions. The emissive behaviour in organic solvent of similar compounds, holding a preformed six-membered ring through hydrogen bonding between the phenol hydroxy group and the C=N bond, enabling under photoirradiation, a phenol-keto tautomerisation in the excited state, was found to occur as a result of the process called ESIPT [9]. Our new compound could *a priori* form three such six-memberred rings (Fig. 1) through hydrogen bonding i.e. two rings formed with the participation of marginal phenol groups and the carbonyl groups and one involving the central phenol group and the double bond nitrogen; this suggested an interesting behaviour in the presence of stimuli such as solvent and light. Indeed, screening of the emission in DMSO at 10^{-4} M indicated a significant different behaviour of compound **1**. The fluorescence spectrum showed an emission maximum at λ_{em} = 562 nm, when excitation was performed at λ_{exc} = 370 nm and an emission maximum at λ_{em} = 530 nm upon excitation at λ_{exc} = 458 nm (Fig. 2). Differences in the absorption and excitation spectra (Fig. 2, λ_{em} = 562 nm) as well as the very large Stokes shift (almost 200 nm, 9.23 × 10^{-4} cm^{-1}) and variation of the emission wavelength according to excitation confirmed occurrence of the ESIPT process [9]. In addition, the spectra had a different pattern compared to spectra of compounds bearing only one hydroxyl group (see also SI for spectra of the benzyl-protected compound **1-OBn**). This observation could be an indication of a more complicated mechanism of light emission, as a consequence of the structural particularities, considering that the hydrazone bonds are susceptible to photoirradiation and, besides configurational modifications, different conformational equilibria could be present in solution, especially since there are three preformed six-memberred rings which could undergo ESIPT.

We have further focused on the behaviour of **1** in aqueous environment. Addition of increasing amounts of water to solutions of **1** in DMSO yielded emission spectra (Fig. 2) which indicated a change in the emitted light from green to yellow, with a red shift in the emission maxima of approximately 30 nm at 90% water content (λ_{em} = 592 nm, λ_{exc} = 370 nm, see SI, Table S1). The ESIPT seemed no longer active at higher water contents and AIE was most probably responsible for the yellow-orange emitted colour [10]. The emission maxima became independent of the excitation wavelength for solutions containing higher water percentages (Fig. 2). These results suggested that compound **1** could also act as switchable-light emissive molecule, triggered by light and/or solvent [8a]. We have also performed solid state fluorescence of compound **1** (SI, Figure S5) which showed a sharp emission band at λ_{em} = 560 nm upon excitation at λ_{exc} = 480 nm.

3.2. Response to pH

To further characterise the response of compound **1** to various aqueous environments, we set in to qualitatively test a wide range of anionic analytes (carbonate, bicarbonate, hydrogen phosphate, dihydrogen phosphate, sulphate, thiocyanate, cyanate, thioacetate, acetate, chloride, iodide, fluoride, bromide, nitrate, nitrite, iodate, bromate, azide) in DMSO/water = 1/9, v/v (SI, Figure S6). We noticed a change in colour from yellow-orange to green for carbonate, bicarbonate, dihydrogen phosphate and fluoride, as well as a very large enhancement of the green emission in presence of the hydroxide ions. Subsequent titration with increasing amounts of aqueous sodium hydroxide generated a blue shift of the emission maximum from λ_{em} = 590 nm to λ_{em} = 545 nm (λ_{exc} = 370 nm) along with the emission band sharpening and, most importantly, a large fluorescence enhancement (approximately 100 fold) above the stoichiometry equivalence (Fig. 3A).

Next, we studied the fluorescence response to variation of pH, by measuring the emission spectra in buffers between pH = 6.0 and pH = 10.6 (Fig. 3B). Increase of the pH led to a blue shift in the emission maximum, concomitant to an increase of the fluorescence intensity and an additional increase of the band at λ_{em} = 420 nm. Plot of I_{590}/I_{520} versus pH values yielded two inflexion points that indicated the corresponding ionisation steps around 7.0 and 8.9.

To understand the structural variations of **1** under the aqueous environmental changes, we performed NMR experiments. We previously found [8a] that under light irradiation or by addition of water, conformation of the hydroxyphenyl-bis-*N*-acylhydrazones underwent a reversible change between three possible conformations (I/II/III in SI, Figure S8), with *E* configuration of the C=N bond, which caused the emitted colour modification from green to yellow. These results were also confirmed for compound **1** by recording ^{1}H NMR spectra in DMSO-d_6 and mixtures of DMSO- D_2O as well as 2D NMR spectra (COSY-HH and NOESY, see SI, Figures S9,S10 for details regarding the assignment of signals to the proposed conformation, under *E* configuration of the C=N double bond in pure organic solvent and mixtures

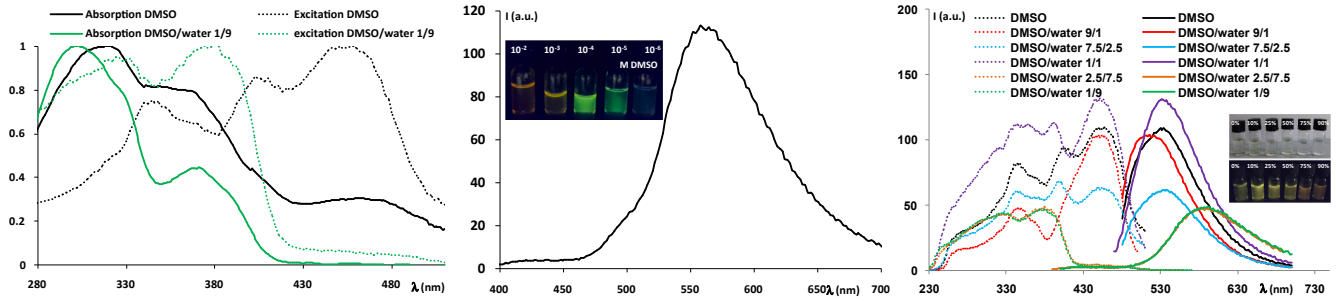

Fig. 2. Left: Normalized absorption and excitation spectra of **1** in DMSO and mixture of DMSO/water 1/9; **Middle**: Emission spectra of 10^{-4} M **1** in DMSO at λ_{exc} = 365 nm. **Photo**: various concentrations of compound **1** in DMSO under UV light (365 nm); **Right**: Excitation and emission spectra of 10^{-4} M **1** in DMSO and various mixtures of DMSO and water. **Photo**: solutions of **1** (10^{-4} M) at various water percentages in DMSO, under day light (up) and UV light (bottom, λ_{exc} = 365 nm).

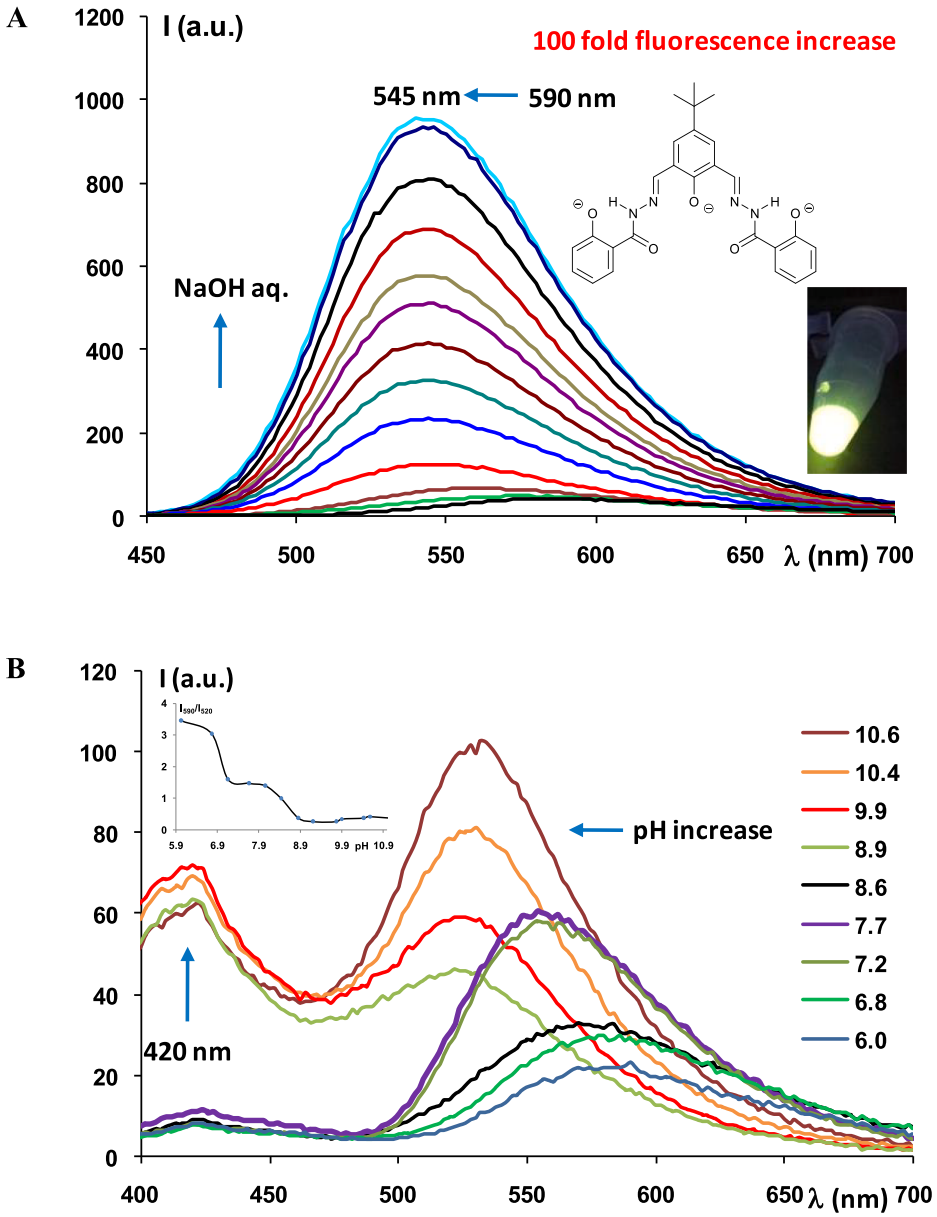

Fig. 3. A: Emission spectra (λ_{exc} = 370 nm) of **1** (10^{-4} M final concentration in 1% DMSO in water) upon addition of increasing amounts of NaOH (up to 80 equivalents with respect to **1**). Inset: proposed structure of **1** at basic pH. **B**: Emission spectra (λ_{exc} = 370 nm) of **1** (10^{-4} M final concentration) in buffers of different pH values (from 6.0 to 10.6). Inset: plot of the I_{590}/I_{520} ratio versus pH.

with deuterated water). We further investigated the structural changes noted by addition of the hydroxide ions, which triggered a bright green fluorescence (Fig. 3, photo). The presence of three phenol hydroxyl groups generated more complex equilibria in solution, cumbering the precise assignment of the species responsible with the emission of light. However, we could conclude that the possible conformation under *E* configuration of the double bond is stabilized by the addition of water (species III in SI, Figure S8), as inferred from 2D NMR spectra (SI, Figure S11, indicating long distance couplings between phenyl and imine protons). We could also assume that species in Fig. 3A (species IV in SI, Figure S8) could be the most probable species resulted following addition of hydroxide ions and the green light might be a consequence of the net negative charges which could induce ESIPT, under photo-irradiation, through hydrogen bonding with the NH groups of the hydrazide moieties.

3.3. Cell staining

The optical properties of **1** prompted the idea that it may be used as a fluorescent stain for biological systems. We therefore used the model eukaryote microorganisms *Saccharomyces cerevisiae* to determine the interaction between **1** and yeast cells. For this purpose, exponentially-growing yeast cells were exposed to **1** added from a 10^{-2} M DMSO stock to final concentrations ranging from 10^{-5} M to 5×10^{-4} M; this corresponded to a maximum 1% DMSO, completely non-toxic to yeast cells (SI, Figure S12). It was noted that at the concentrations used, **1** did not affect significantly the proliferation rate or the viability of yeast cells (data not shown). Moreover, **1** even stimulated cell proliferation when used at 10^{-4} M, final concentration. Yeast cells exposed to **1** were also observed by florescence microscopy. It was noticed that UV-excited yeast cells (in the 340–390 nm wavelength band) became fluorescent after 10 s of UV exposure (Fig. 4); the fluorescence pattern indicated

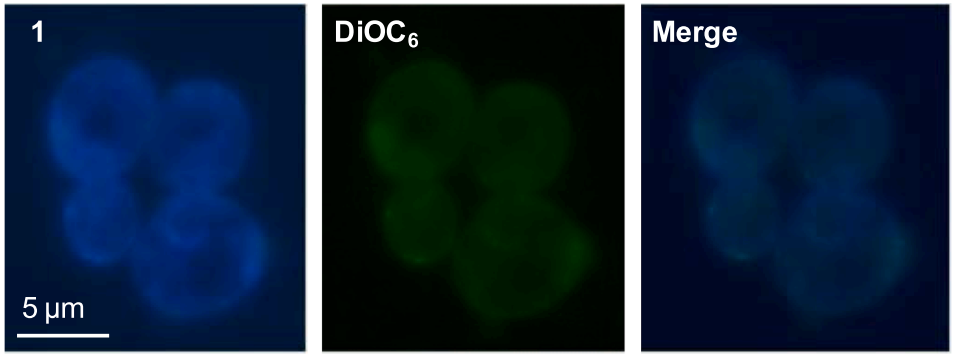

Fig. 4. Effect of **1** on *S. cerevisiae* cells. BY4741 yeast cells were inoculated in SD liquid medium and grown to density 10^6 cells/mL before addition of **1**. Co-staining with **1** and $DiOC_6$ reveals that **1** stains the perinuclear and ER membrane. Cells were visualized by fluorescence microscopy (λ_{exc} = 340–390 nm, λ_{em} = 420 nm for **1**; λ_{exc} = 470–495 nm, λ_{em} = 510–550 nm for $DiCO_6$).

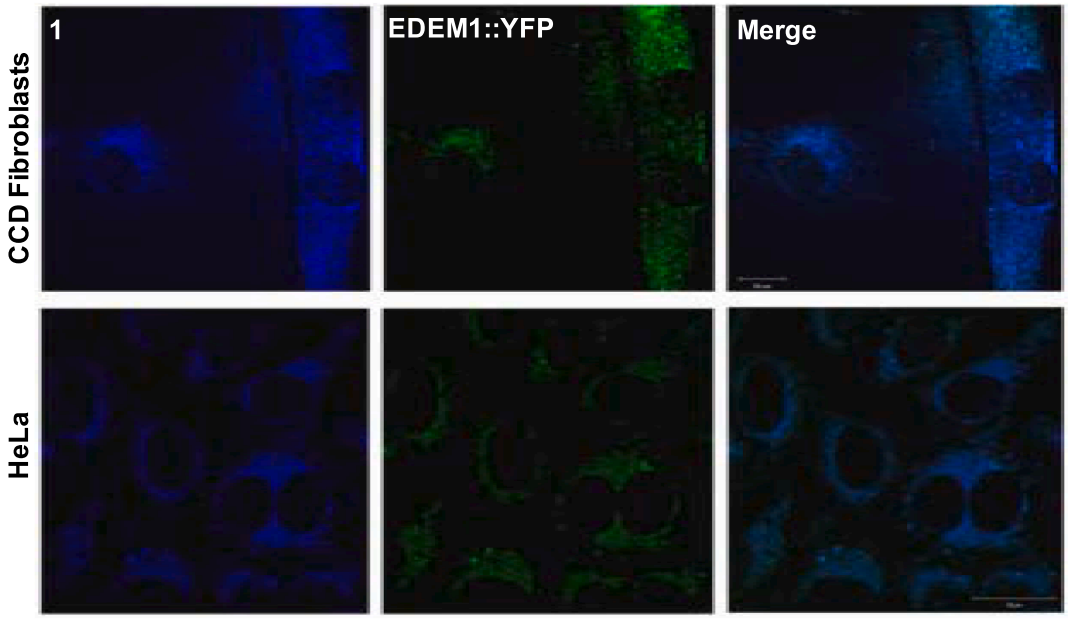

Fig. 5. Confocal fluorescent images of fibroblasts and HeLa cells expressing EDEM1::YFP and stained by **1**. Representative micrographs of other independent experiments are presented in SI.

that **1** accumulated at the perinuclear-endoplasmic reticulum (ER) level, as shown by co-staining with $DiOC_6$ (3,3′-dihexyloxacarbocyanine iodide). This is a cell permeable green fluorescent lipophilic dye which is used to highlight ER in yeast cells [15], absorbs at 485 nm and emits at 502 nm, therefore no significant overlapping between $DiOC_6$ and **1** was expected. Indeed, when visualising the **1**-stained yeast cells using the filter set used for $DiOC_6$, no fluorescence could be detected (data not shown). Co-staining yeast cells with **1** and $DiOC_6$ revealed that both dyes accumulated at the perinuclear-ER level (Fig. 4). It is possible that binding of **1** to internal membranes results in florescence enhancement; in this line of evidence, it was noted that lecithin, the most abundant membrane glycerophospholipid, augmented the fluorescence intensity of **1** (SI, Figure S12). Moreover, experiments performed using the benzyl-protected compound **1-OBn** (see SI for structure and characterisation) did not reveal any labelling (data not shown), suggesting that presence of the hydroxyl groups are mandatory for this selective ER visualization.

Next, we assessed the efficiency of **1** dye in binding ER membranes in mammalian cells. For this purpose, CCD fibroblast and HeLa cells, two models of normal and cancer immortalized cell lines, were exposed for two hours to a final concentration of 10^{-4} M **1** before live cells were imaged by confocal microscopy. It was noted that in both cell types the dye showed a reticulate pattern with a perinuclear concentration (Fig. 5 and SI), similar to ER morphology.

To verify whether the staining given by **1** is specific for ER network, EDEM1 fused to yellow fluorescent protein, YFP (EDEM1::YFP) was used as marker for ER. EDEM1 is a protein involved in ERAD (Endoplasmic Reticulum Associated Degradation) in mammalian cells and it localizes to the ER under normal conditions. [16] The cells were transiently transfected with the plasmid harboring EDEM1::YFP and 24 h post transfection the cells were incubated with 10^{-4} M solution of **1** and imaged by confocal microscopy as above. In both cell lines, **1** stained the reticulate structures spanning the cytoplasm that also expressed EDEM1:YFP (Fig. 5). The degree of signal overlapping was estimated by measuring two co-localization coefficients. The overlap coefficients according to Manders, which indicate the actual overlap of the signal, were 0.94 for CCD fibroblasts and 0.86 for HeLa cells, whereas the Pearson's correlation coefficients, which describe the correlation of the intensity distribution between channels, were 0.74 and 0.68, respectively [17]. These values suggested extended co-localization between signals. Of note, the **1** concentrations used were not toxic and did not significantly affect cell viability (SI, Figure S13).

4. Conclusions

We described the synthesis and characterisation of a new hydroxy-bis-*N*-acylhydrazone which acts as multiple light emissive probe in organic and aqueous environments. We investigated the fluorescence response at different pH values and assigned the emission colour switching by conformation modifications, as inferred from NMR

experiments. Further, the probe was able to target ER membranes in eukaryote microorganisms (*Saccharomyces cerevisiae*) and mammalian cells (CCD fibroblast and HeLa), suggesting it can be used for live labelling of ER. Overall, our compound can have applicative potential as it can be obtained by a straightforward synthetic procedure, has reduced cytotoxic action, is chemically stable in aqueous environments and completely inert to the intracellular activity. In addition, the blue emission around 420 nm allows the use filter sets routinely used in fluorescence microscopy, with excitation wavelengths between 340 and 390 nm. The availability of the *N*-acylhydrazone for imaging of living cells prompt for further structural diversification in order to shift the emission of light toward longer wavelengths.

Acknowledgements

We are grateful to Lavinia Ruta and Simona Ghenea for testing the effect of **1** on cell growth and viability. M.M. acknowledges project no. PN-II-RU-TE-2014-4-0808 and the University of Bucharest for partial funding of this work.

Appendix A. Supplementary material

Supplementary data to this article can be found online at https://doi.org/10.1016/j.bioorg.2019.103295.

References

[1] (a) J.M. Lehn, Perspectives in chemistry—aspects of adaptive chemistry and materials, Angew. Chem. Int. Ed. 54 (2015) 3276–3289, https://doi.org/10.1002/anie.201409399;
(b) M. Matache, E. Bogdan, N.D. Hădade, Selective host molecules obtained by dynamic adaptive chemistry, Chem. Eur. J. 20 (2014) 2106–2131, https://doi.org/10.1002/chem.201303504.

[2] (a) I. Aprahamian, Hydrazone switches and things in between, Chem. Commun. 53 (2017) 6674–6684, https://doi.org/10.1039/c7cc02879b;
(b) L. Tatum, L.A. Tatum, X. Su, I. Aprahamian, Simple hydrazone building blocks for complicated, ACC Chem. Res. 47 (2014) 2141–2149, https://doi.org/10.1021/ar500111f.

[3] A.M. Stadler, J. Harrowfield, Bis-acyl-/aroyl-hydrazones as multidentate ligands, Inorg. Chim. Acta 362 (2009) 4298–4314, https://doi.org/10.1016/j.ica.2009.05.062.

[4] (a) C.C. Paraschivescu, N.D. Hədade, A.G. Coman, A. Gautier, F. Cisnetti, M. Matache, Symmetrical and non-symmetrical 2,5-diaryl-1,3,4-oxadiazoles: synthesis and photophysical properties, Tetrahedron. Lett. 56 (2015) 3961–3964, https://doi.org/10.1016/j.tetlet.2015.05.005;
(b) A. Paun, C.C. Paraschivescu, M. Matache, V.I. Parvulescu, Synthesis of new alkynyl-bridged 2,5-disubstituted 1,3,4-oxadiazoles, Synth 48 (2016) 606–614, https://doi.org/10.1055/s-0035-1560387;
(c) W. Yu, G. Huang, Y. Zhang, H. Liu, L. Dong, X. Yu, Y. Li, J. Chang, I2-mediated oxidative C-O bond formation for the synthesis of 1,3,4-oxadiazoles from aldehydes and hydrazides, J. Org. Chem. 78 (2013) 10337–10343, https://doi.org/10.1021/jo401751h.

[5] (a) S.Y. Lin, L. Zhao, Y.N. Guo, P. Zhang, Y. Guo, J. Tang, Two new Dy3 triangles with trinuclear circular helicates and their single-molecule magnet behavior, Inorg. Chem. 51 (2012) 10522–10528, https://doi.org/10.1021/ic300371m;
(b) S.Y. Lin, G.F. Xu, L. Zhao, Y.N. Guo, Y. Guo, J. Tang, Observation of slow magnetic relaxation in triple-stranded lanthanide helicates, Dalton Trans. 40 (2011) 8213–8217, https://doi.org/10.1039/C1DT10729A;
(c) S.S. Beloborodov, S.I. Levchenkov, L.D. Popov, V.V. Lukov, I.N. Shcherbakov, G.G. Alexandrov, V.A. Kogana, Crystal structure and magnetic properties of binuclear DyIII complexes with 4-substituted 2,6-diformylphenol bis (acylhydrazones), Mendeleev Commun. 24 (2014) 219–221, https://doi.org/10.1016/j.mencom.2014.06.010;
(d) K. Das, S. Nandi, S. Mondal, T. Askun, Z. Cantuk, P. Celikboyun, C. Massera, E. Garribba, A. Datta, C. Sinha, T. Akitsug, Triply phenoxo bridged Eu(III) and Sm(III) complexes with 2,6-diformyl-4-methylphenol-di(benzoylhydrazone): structure, spectra and biological study in human cell lines, New. J. Chem. 39 (2015) 1101–1114, https://doi.org/10.1039/C4NJ01464B;
(e) F.B. Tamboura, O. Diouf, A.H. Barry, M. Gaye, A.S. Sall, Dinuclear lanthanide (III) complexes with large-bite Schiff bases derived from 2,6-diformyl-4-chlorophenol and hydrazides: synthesis, structural characterization and spectroscopic studies, Polyhedron 43 (2012) 97–103, https://doi.org/10.1016/j.poly.2012.06.025.

[6] (a) S. Anbu, E.C.B.A. Alegria, A.J.L. Pombeiro, Catalytic activity of a benzoyl hydrazone based dimeric dicopper(II) complex in catechol and alcohol oxidation reactions, Inorg. Chim Acta 431 (2015) 139–144, https://doi.org/10.1016/j.ica.2014.11.038;
(b) M.R. Maurya, S. Dhaka, F. Avecilla, Oxidation of secondary alcohols by conventional and microwave-assisted methods using molybdenum complexes of ONO donor ligands, New J. Chem. 39 (2015) 2130–2139, https://doi.org/10.1039/C4NJ02208D.

[7] (a) T. Mistri, M. Dolai, D. Chakraborty, A.R. Khuda-Bukhsh, K.K. Das, M. Ali, A highly selective and sensitive in vivo fluorosensor for zinc(ii) without cytotoxicity, Org. Biomol Chem. 10 (2012) 2380–2384, https://doi.org/10.1039/c2ob07084g;
(b) S. Anbu, R. Ravishankaran, M.F.C. Guedes da Silva, A.A. Karande, A.J.L. Pombeiro, Differentially selective chemosensor with fluorescence off–on responses on Cu^{2+} and Zn^{2+} ions in aqueous media and applications in pyrophosphate sensing, live cell imaging, and cytotoxicity, Inorg. Chem. 53 (2014) 6655–6664, https://doi.org/10.1021/ic500313m;
(c) S. Anbu, S. Kamalraj, C. Jayabaskaran, P.S. Mukherjee, Naphthalene carbohydrazone based dizinc(II) chemosensor for a pyrophosphate ion and its DNA assessment application in polymerase chain reaction products, Inorg. Chem. 52 (2013) 8294–8296, https://doi.org/10.1021/ic4011696.

[8] (a) A.G. Coman, A. Paun, C.C. Popescu, N.D. Hădade, C.C. Anghel, A.M. Mădălan, P. Ionita, M. Matache, Conformation-induced light emission switching of N -acylhydrazone systems, New J. Chem. 42 (2018) 14111–14119, https://doi.org/10.1039/C8NJ01880D;
(b) A. Maity, F. Ali, H. Agarwalla, B. Anothumakkool, A. Das, Tuning of multiple luminescence outputs and white-light emission from a single gelator molecule through an ESIPT coupled AIEE process, Chem. Commun. 51 (2015) 2130–2133, https://doi.org/10.1039/c4cc09211b.

[9] (a) A.C. Sedgwick, L. Wu, H.-H. Han, S.D. Bull, X.-P. He, T.D. James, et al., Excited-state intramolecular proton-transfer (ESIPT) based fluorescence sensors and imaging agents, Chem. Soc. Rev. 47 (2018) 8842–8880, https://doi.org/10.1039/C8CS00185E;
(b) J.E. Kwon, S.Y. Park, Advanced organic optoelectronic materials: Harnessing excited-state intramolecular proton transfer (ESIPT) process, Adv. Mater. 23 (2011) 3615–3642, https://doi.org/10.1002/adma.201102046.

[10] (a) J. Mei, N.L.C. Leung, R.T.K. Kwok, J.W.Y. Lam, B.Z. Tang, Aggregation-Induced Emission: Together We Shine, United We Soar! Chem. Rev. 115 (2015) 11718–11940. doi: 10.1021/acs.chemrev.5b00263. (b) Feng G, Kwok RTK, Tang BZ, Liu B, Functionality and versatility of aggregation-induced emission luminogens, Appl. Phys. Rev. 4 (2017) 021307–021341. doi: 10.1063/1.4984020. (c) D. Ding Aggregation-induced emission luminogens for biomedical applications, In: Y. Tang, B. Tang (Eds.), Principles and Applications of Aggregation-Induced Emission, 2019, 457–478. Springer, Cham.

[11] (a) For selected, relevant reviews, see: E.W. Miller, C.J. Chang, Fluorescent probes for nitric oxide and hydrogen peroxide in cell signaling, Curr. Opin. Chem. Biol. 11 (2007) 620–625, https://doi.org/10.1016/j.cbpa.2007.09.018;
(b) D. Wu, A.C. Sedgwick, T. Gunnlaugsson, E.U. Akkaya, J. Yoon, T.D. James, Fluorescent chemosensors: the past, present and future, Chem. Soc. Rev. 46 (2017) 7105–7123, https://doi.org/10.1039/c7cs00240h;
(c) P.A. Gale, C. Caltagirone, Fluorescent and colorimetric sensors for anionic species, Coord. Chem. Rev. 354 (2018) 2–27, https://doi.org/10.1016/j.ccr.2017.05.003;
(d) C.P. Satori, M.M. Henderson, E.A. Krautkramer, V. Kostal, M.M. Distefano, E.A. Arriaga, Bioanalysis of eukaryotic organelles, Chem. Rev. 113 (2013) 2733–2811, https://doi.org/10.1021/cr300354g;
(e) W. Xu, Z. Zeng, J.H. Jiang, Y.T. Chang, L. Yuan, Discerning the chemistry in individual organelles with small-molecule fluorescent probes, Angew Chemie – Int Ed 55 (2016) 13658–13699, https://doi.org/10.1002/anie.201510721;
(f) Kumar N Roopa, V. Bhalla, M. Kumar, Development and sensing applications of fluorescent motifs within the mitochondrial environment, Chem. Commun. 51 (2015) 15614–15628, https://doi.org/10.1039/c5cc07098h;
(g) Y. Yue, F. Huo, S. Lee, C. Yin, J. Yoon, A review: the trend of progress about pH probes in cell application in recent years, Analyst 142 (2017) 30–41, https://doi.org/10.1039/c6an01942k;
(h) S.H. Alamudi, Y.-T. Chang, Advances in design of cell-permeable fluorescent probe for applications in live cell imaging, Chem. Commun. 54 (2018) 13641–13653, https://doi.org/10.1039/C8CC08107G.

[12] L.D. Lavis, R.T. Raines, Bright ideas for chemical biology, ACS Chem. Biol. 3 (2008) 142–155, https://doi.org/10.1021/cb700248m.

[13] J. Wu, W. Liu, J. Ge, H. Zhang, P. Wang, New sensing mechanisms for design of fluorescent chemosensors emerging in recent years, Chem. Soc. Rev. 40 (2011) 3483–3495, https://doi.org/10.1039/c0cs00224k.

[14] (a) J.M. Meinig, L. Fu, B.R. Peterson, Synthesis of fluorophores that target small molecules to the endoplasmic reticulum of living mammalian cells, Angew. Chemie. Int. Ed. 54 (2015) 9696–9699 10.1002/anie.201504156;
(b) T. Zou, C.N. Lok, Y.M.E. Fung, C.M. Che, Luminescent organoplatinum(ii) complexes containing bis(N-heterocyclic carbene) ligands selectively target the endoplasmic reticulum and induce potent photo-toxicity, Chem. Commun. 49 (2013) 5423–5425, https://doi.org/10.1039/c3cc40953h;
(c) J.S. Nam, M.G. Kang, J. Kang, S.Y. Park, S.J.C. Lee, H.T. Kim, et al., Endoplasmic reticulum-localized iridium(III) complexes as efficient photodynamic therapy agents via protein modifications, J. Am. Chem. Soc. 138 (2016) 10968–10977, https://doi.org/10.1021/jacs.6b05302;
(d) H. Zhang, J. Fan, H. Dong, S. Zhang, W. Xu, J. Wang, P. Gao, X. Peng, Fluorene-derived two-photon fluorescent probes for specific and simultaneous bioimaging of endoplasmic reticulum and lysosomes: group-effect and localization, J. Mater. Chem. B 1 (2013) 5450–5455, https://doi.org/10.1039/C3TB20646G;
(e) S.K. Verma, P. Kumari, S.N. Ansari, M.O. Ansari, D. Deori, S.M. Mobin, A novel mesoioniccarbene based highly fluorescent Pd(II) complex as an endoplasmic reticulum tracker in live cells, Dalton Trans. 47 (2018) 15646–15650, https://doi.

org/10.1039/C8DT02778A;
(f) P. Kumari, S.K. Verma, S.M. Mobin, A facile two-photon fluorescent probe: an endoplasmic reticulum tracker monitoring ER stress and vesicular transport to lysosomes, Chem. Commun. (2018) 2–5 2019/CC/C8CC07429A.

[15] A.J. Koning, P.Y. Lum, J.M. Williams, R. Wright, DiOC6 staining reveals organelle structure and dynamics in living yeast cells, Cell Motil Cytoskeleton 25 (1993) 111–128, https://doi.org/10.1002/cm.970250202.

[16] (a) N. Hosokawa, I. Wada, K. Hasegawa, T. Yorihuzi, L.O. Tremblay, A. Herscovics, K. Nagata, A novel ER alpha-mannosidase-like protein accelerates ER-associated degradation, EMBO Rep. 2 (2001) 415–422, https://doi.org/10.1093/embo-reports/kve084;
(b) M. Molinari, V. Calanca, C. Galli, P. Lucca, P. Paganetti, Role of EDEM in the release of misfolded glycoproteins from the calnexin cycle, Science 299 (2003) 1397–1400, https://doi.org/10.1126/science.1079474.

[17] V. Zinchuk, O. Zinchuk, T. Okada, Quantitative colocalization analysis of multicolor confocal immunofluorescence microscopy images: pushing pixels to explore biological phenomena, Acta Histochem. Cytochem. 40 (2007) 101–111, https://doi.org/10.1267/ahc.07002.